International Electronic Journal of Geometry
Volume 4 No. 2 pp. 63–84 (2011) ©IEJG

GEOMETRIC INVARIANTS OF PARAMETRIC TRIANGULAR QUADRIC PATCHES

GUDRUN ALBRECHT

(Communicated by Kazım ILARSLAN)

Abstract. The paper presents a geometric solution to the problem of extracting the geometric invariants of a quadric that is represented in parametric rational quadratic triangular Bézier form. The starting point of the presented method is the algorithm given in [3], that established whether a given rational quadratic Bézier triangle describes a quadric, and in the affirmative case also determined the quadric's affine type; on this basis, the present algorithm additionally determines the quadric's axes, thus providing the coordinate system with respect to which the patch's underlying quadric has normal form.

1. Introduction

Both, rational triangular parametric Bézier surfaces as well as quadric surfaces are important primitives in Computer Aided Geometric Design applications, see, e.g., [11].

On the one hand, among n–sided parametric surface patches [12, 24] the most promising and flexible shape for the description of complex geometries seems to be the triangular one, see, e.g., [13]. *Rational* triangular Bézier patches are more flexible than polynomial Bézier triangles and contain the latter ones as special cases. The higher flexibility is due to the so–called *weights*, which are additional design elements; see e.g. [1, 2, 22] for a geometrical interpretation of these weights.
On the other hand, quadric surfaces, i.e., spheres, cones, cylinders, ellipsoids, hyperboloids, and paraboloids, are very popular in applications such as mechanical engineering and architecture due to their appealing and practical shapes as well as their simple implicit and parametric representations.

In order to benefit from the advantages of both of the above mentioned surface representations several authors have addressed the problem of relating quadric surfaces and rational parametric Bézier triangles. It turned out, that the lowest degree for a rational triangular parametric Bézier surface to describe a quadric is two. These quadratic rational Bézier triangles in general describe so–called Steiner

2000 *Mathematics Subject Classification.* 51N15, 51N20, 68U05, 68U07, 65D17, 65D18.
Key words and phrases. rational triangular quadratic Bézier patch, quadric, geometric invariants, quadric's axes.

surfaces, which are algebraic surfaces of order four that comprise the second order quadric surfaces, see, e.g., [21, 19, 10, 9].

Unlike the curve case, where there is a one–to–one correspondence between rational parametric curves of degree two and second order algebraic curves or conic section, see, e.g, [11], in the surface case the control points and the weights of the rational quadratic Bézier triangle thus have to satisfy certain conditions for the patch to represent a quadric. One necessary condition for a rational quadratic Bézier triangle to describe a non–degenerate quadric consists in its boundary conics meeting in one point, the center of the stereographic projection that is reciprocal to the parametrisation. All existing criteria, see [7, 8, 18, 14, 17, 15, 16] are of theoretical nature or involve implicitization of the quadric, see [21].

An easy, practical and geometry driven algorithm for the problem of determining whether a given rational triangular quadratic Bézier patch lies on a quadric surface or not has been presented in [3], and has thoroughly been investigated from the numerical point of view in [4]. The decision of whether the given patch represents a quadric or not is based on the theoretical classification [10] of rational triangular Bézier surfaces of degree two. Once a given patch is found to describe a quadric, the quadric's affine type is established. First, the Gaussian curvature is used for a rough classification yielding the projective type of the quadric. Next, the type of the quadric's intersection with the plane at infinity helps to determine the desired affine type.

The purpose of the present article is to complete the algorithm from [3] by, in the case of a quadric patch, additionally providing the quadric's axes. In this way it is thus possible to first test whether a given rational quadratic triangular Bézier patch represents a quadric, and then to step by step geometrically recover its geometric invariants that allow to fully describe the patch's underlying quadric.

The paper is organized as follows. In section 2 we formulate the problem and summarize the results from [3] as far as they are necessary for the extraction of the quadric's geometric invariants. Then, in section 3, based on a result from classical geometry, we determine the axes directions of the underlying quadric. On this basis, section 4 is then devoted to determining the position of the origin $\mathbf{o}$ such that, in the coordinate system given by $\mathbf{o}$ and the three axes directions, the quadric has normal form. In section 5 we illustrate the algorithm for several significant examples, and we conclude in section 6.

2. Formulation of the problem and preliminaries

We are given a non–planar rational triangular Bézier patch of degree 2

$$\mathbf{B} : \mathbf{x}(u,v,w) = \frac{\sum_{i+j+k=2} w_{ijk}\mathbf{b}_{ijk}B^2_{ijk}(u,v,w)}{\sum_{i+j+k=2} w_{ijk}B^2_{ijk}(u,v,w)} \in I\!R^3 \tag{2.1}$$

where (u,v,w) are barycentric coordinates $(u+v+w=1)$, and $B^2_{ijk}(u,v,w) = 2!/(i!j!k!)u^iv^jw^k$ are Bernstein polynomials. $\mathbf{b}_{ijk} = (b^1_{ijk}, b^2_{ijk}, b^3_{ijk})^T \in I\!R^3$ are the control points and $w_{ijk} \in I\!R^+ \setminus \{0\}$ the weights. In the remainder of this paper the normalization $u+v+w=1$ may be omitted if necessary, the coordinates thus being interpreted as homogeneous (complex) coordinates $(u:v:w)$ of the entire projective plane.

In general, such a patch describes an algebraic surface of order four, the so–called Steiner surface. These Steiner surfaces comprise quadric surfaces for special configurations of the control points and the weights, see [3] and references cited therein. In [3] a simple and practical algorithm has been presented in order to decide, from the given parametrisation (2.1), whether the patch describes a quadric or not, and if so, to determine the quadric's affine type. For a patch, that we know to lie on a quadric, a natural problem then consists in determining the quadric's axes directions $\mathbf{d}_1, \mathbf{d}_2, \mathbf{d}_3$ as well as the position of the origin $\mathbf{o}$ such that, with respect to the coordinate system $\{\mathbf{o}; \mathbf{d}_1, \mathbf{d}_2, \mathbf{d}_3\}$, the underlying quadric is in canonical position (see [23] for a list of the canonical or normal forms of quadrics in Euclidean 3–space.) In order to solve the problem of determining the quadric's axes directions and the appropriate position of the origin from the given parametrisation (2.1) we will base our considerations on the classification presented in [3]. We thus suppose the parameter representation (2.1), which may be written as

$$\mathbf{x}(u,v,w) = \Big(\frac{x_1(u,v,w)}{x_0(u,v,w)}, \frac{x_2(u,v,w)}{x_0(u,v,w)}, \frac{x_3(u,v,w)}{x_0(u,v,w)}\Big)^T, \tag{2.2}$$

to desribe a quadric surface Q. It may be interpreted as a rational quadratic map from the uvw–parameter plane ϵ onto the quadric Q, and thus as the inverse of a stereographic projection σ of Q onto ϵ (see [3]). According to [18], only in the case of degenerate quadrics (Gaussian curvature $K = 0$) there exist exceptional rational quadratic Bézier patches which do not define a stereographic projection; this case is omitted here.

In the case of a *non–degenerate* quadric (Gaussian curvature $K \neq 0$) the stereographic projection σ is characterized by the projection center $\mathbf{z} \in Q$ and two degeneration points or base points $\mathbf{p}_1, \mathbf{p}_2$. Their connecting line is referred to as degeneration line or base line L_{12} of σ and is obtained as intersection of the tangent plane $T_{\mathbf{z}}$ of Q in $\mathbf{z}$ with ϵ. $\mathbf{p}_1$ and $\mathbf{p}_2$ lie on the intersection lines t_1 and t_2 of Q and $T_{\mathbf{z}}$ respectively. With exception of the degeneration points $\mathbf{p}_1, \mathbf{p}_2$ and the projection center $\mathbf{z}$ the map σ establishes a one–to–one correspondence between points on the quadric Q and points in the parameter plane ϵ. Analytically, the exceptional role of the points $\mathbf{p}_i(u_i, v_i, w_i) \in \epsilon$ $(i = 1, 2)$ is equivalent to the fact, that all four conic sections $x_j(u,v,w) = 0$, $j = 0, 1, 2, 3$ intersect in the points $\mathbf{p}_1, \mathbf{p}_2$.

The situation in the case of a *degenerate* quadric Q (Gaussian curvature $K = 0$) is obtained from the above one by simply considering that the tangent plane $T_{\mathbf{z}}$ in $\mathbf{z}$ ($\neq$ singularity of Q) intersects Q in a double line t and thus the above two degeneration points $\mathbf{p}_1, \mathbf{p}_2$ become one double point $\mathbf{p} := t \cap \epsilon$ and the degeneration line L touches Q in $\mathbf{p}$.

For the following considerations it is sometimes convenient to projectively expand Euclidean 3–space into projective 3–space $I\!P^3$. By doing so a point $\mathbf{x}(x, y, z)$ will be represented by homogeneous coordinates $\mathbf{X}(x_0, x_1, x_2, x_3)$, and the relation between the affine and the projective coordinates is given by

$$x = \frac{x_1}{x_0}\,,\; y = \frac{x_2}{x_0}\,,\; z = \frac{x_3}{x_0} \tag{2.3}$$

for $x_0 \neq 0$. The points with $x_0 = 0$ form a plane, the so–called plane at infinity, which we will refer to by η. Thus, projective 3–space $I\!P^3$ is obtained from Euclidean 3–space by adding η to it. We denote points and directions in Euclidean 3–space

by bold face letters $\mathbf{p}, \mathbf{q}, \mathbf{y}, \mathbf{d}, \ldots$, and points in projective 3–space by capital bold face letters $\mathbf{P}, \mathbf{Q}, \mathbf{X}, \mathbf{Y}, \ldots$.

Depending on the position of the plane at infinity η with respect to the quadric Q (η/Q) and with respect to the center $\mathbf{z}$ of the stereographic projection ($\eta/\mathbf{z}$) an affine classification of the quadric Q has been derived in [3]. It depends on the type of the stereographic projection $\sigma(k_\eta)$ of the quadric's conic at infinity $k_\eta = Q \cap \eta$, which, being a conic itself, is given by the equation

$$\sigma(k_\eta): \quad x_0(u,v,w) = \sum_{i+j+k=2} w_{ijk} B_{ijk}^2(u,v,w) = 0. \tag{2.4}$$

This classification is summarized in tables 1 and 2. Table 1 contains all possible cases for non–degenerate quadrics, i.e., ellipsoids, hyperboloids and paraboloids, whereas table 2 displays all possible configurations for degenerate quadrics, i.e., cones and cylinders. In table 1, last column, K denotes the Gaussian curvature whose sign is the same in all points of the quadric. In table 2, $\mathbf{s}$ denotes the vertex of the cone or cylinder, where $\mathbf{s} \notin \epsilon$, and $\eta/\mathbf{s}$ stands for η's position with respect to $\mathbf{s}$.

Based on this affine classification in the following section we solve the problem of determining the axes directions of the quadric Q given in its parameter form (2.1).

3. Determination of the principal axes directions

3.1. **General situation.** The solution of the problem of determining the axes directions of a quadric given in parameter form will be based on a result from classical geometry. We thus first provide the necessary elements for a correct understanding of the situation.

As we have seen in the previous section the plane at infinity η intersects the quadric Q in a conic section, the quadric's conic at infinity, referred to as k_η. The plane at infinity η also contains the so–called absolute conic

$$k_a: \quad x_1^2 + x_2^2 + x_3^2 = 0, \; x_0 = 0, \tag{3.1}$$

which is entirely imaginary.

Given four non–colinear points $\mathbf{P}_1, \mathbf{P}_2, \mathbf{P}_3, \mathbf{P}_4$ on a conic section c we may construct the intersection points $\mathbf{I}_1 = \mathbf{P}_1\mathbf{P}_2 \cap \mathbf{P}_3\mathbf{P}_4$, $\mathbf{I}_2 = \mathbf{P}_1\mathbf{P}_3 \cap \mathbf{P}_2\mathbf{P}_4$, $\mathbf{I}_3 = \mathbf{P}_1\mathbf{P}_4 \cap \mathbf{P}_2\mathbf{P}_3$ of the diagonals of the quadrilateral $\mathbf{P}_1\mathbf{P}_2\mathbf{P}_3\mathbf{P}_4$. The points $\mathbf{I}_k$ and $\mathbf{I}_j$, $k \neq j \in \{1,2,3\}$ are so–called *conjugate* points with respect to the conic c. $\mathbf{I}_k$ is called *pole* of the line $\mathbf{I}_j\mathbf{I}_l$ ($k \neq j, k \neq l, j \neq l$) with respect to c, and $\mathbf{I}_j\mathbf{I}_l$ is the polar (line) of the point $\mathbf{I}_k$ with respect to c. The triangle $\Delta\mathbf{I}_j\mathbf{I}_k\mathbf{I}_l$ is called a *polar* triangle with respect to c. For further information on the theory of poles and polars with respect to conic sections see, e.g., [19, 23].

Based on these preliminaries we thus recall the following theorem from classical projective geometry.

Theorem 3.1. *The task of determining the principal axes of a quadric Q is equivalent to determining the common polar triangle of the quadric's conic at infinity k_η and the absolute conic k_a. The corner points of this triangle determine the principal axes directions of Q.*

Figure 1 illustrates the possible configurations in the plane at infinity. In the general situation (Figure 1, left) Q's conic at infinity k_η and the absolute conic k_a have four distinct intersection points $\mathbf{A} = (0, \mathbf{a}), \bar{\mathbf{A}} = (0, \bar{\mathbf{a}}), \mathbf{B} = (0, \mathbf{b}), \bar{\mathbf{B}} = (0, \bar{\mathbf{b}})$,

case	η/Q	$\eta/\mathbf{z}$	k_η	$\sigma(k_\eta)$	affine type of Q
1	not tangent plane	$\mathbf{z} \notin \eta$	non–degenerate real/imaginary conic section	non–degenerate real/imaginary conic section through $\mathbf{p}_1, \mathbf{p}_2$	hyperboloid of one sheet $(K < 0)$/ ellipsoid $(K > 0)$
2	not tangent plane	$\mathbf{z} \in \eta$	non–degenerate real conic section	real pair of intersecting lines where $L_{12} \subset \sigma(k_\eta)$ and singular point $\notin \{\mathbf{p}_1, \mathbf{p}_2\}$	hyperboloid of one sheet $(K < 0)$ or of two sheets $(K > 0)$
3	tangent plane	$\mathbf{z} \notin \eta$	real/imaginary pair of intersecting lines	real/imaginary pair of intersecting lines l_1, l_2 where $\mathbf{p}_1 \in l_1 \setminus l_2$, $\mathbf{p}_2 \in l_2 \setminus l_1$	hyperbolic $(K < 0)$/ elliptic $(K > 0)$ paraboloid
4	tangent plane	$\mathbf{z} \in \eta$, $\eta \neq T_\mathbf{z}$	real/imaginary pair of intersecting lines	real/imaginary pair of intersecting lines where $L_{12} \subset \sigma(k_\eta)$ and singular point $\in \{\mathbf{p}_1, \mathbf{p}_2\}$	hyperbolic $(K < 0)$/ elliptic $(K > 0)$ paraboloid
5	tangent plane	$\mathbf{z} \in \eta$, $\eta = T_\mathbf{z}$	real/imaginary pair of intersecting lines t_1, t_2	double line L_{12}	hyperbolic $(K < 0)$/ elliptic $(K > 0)$ paraboloid

TABLE 1. Non–degenerate quadric

where $\mathbf{a}, \bar{\mathbf{a}}$ and $\mathbf{b}, \bar{\mathbf{b}}$ denote pairs of conjugate complex triples respectively. In this case, the common polar triangle of k_η and k_a is given by the intersection points $\mathbf{D}_1 = (0, \mathbf{d}_1), \mathbf{D}_2 = (0, \mathbf{d}_2), \mathbf{D}_3 = (0, \mathbf{d}_3)$ of the three pairs of diagonals of the quadrilateral $\mathbf{A}\bar{\mathbf{A}}\mathbf{B}\bar{\mathbf{B}}$. The directions of Q's principal axes are then $\mathbf{d}_1, \mathbf{d}_2, \mathbf{d}_3$.

Figure 1, right, illustrates the situation of a quadric of revolution. In this case the conics k_η and k_a touch each other in two different points $\mathbf{A}(0, \mathbf{a}) = \mathbf{B}(0, \mathbf{b})$ and $\bar{\mathbf{A}}(0, \bar{\mathbf{a}}) = \bar{\mathbf{B}}(0, \bar{\mathbf{b}})$, and their common tangents intersect in a point $\mathbf{D}(0, \mathbf{d})$. $\mathbf{d}$ thus yields the direction of Q's rotation axis.

case	η/Q	$\eta/\mathbf{z}$	$\eta/\mathbf{s}$	k_η	$\sigma(k_\eta)$	affine type of Q
6	not tangent plane	$\mathbf{z} \notin \eta$	$\mathbf{s} \notin \eta$	non–degenerate real conic section	non–degenerate real conic section touching L in $\mathbf{p}$	cone
7	not tangent plane	$\mathbf{z} \notin \eta$	$\mathbf{s} \in \eta$	real/ imaginary pair of intersecting lines	real/imaginary pair of intersecting lines with singular point $\mathbf{p}$ and $L \not\subset \sigma(k_\eta)$	hyperbolic / elliptic cylinder
8	not tangent plane	$\mathbf{z} \in \eta$	$\mathbf{s} \in \eta$	real pair of intersecting lines	real pair of intersecting lines with singular point $\mathbf{p}$ and $L \subset \sigma(k_\eta)$	hyperbolic cylinder
9	not tangent plane	$\mathbf{z} \in \eta$	$\mathbf{s} \notin \eta$	non–degenerate real conic section	real pair of intersecting lines with singular point $\neq \mathbf{p}$ and $L \subset \sigma(k_\eta)$	cone
10	tangent plane	$\mathbf{z} \notin \eta$	$\mathbf{s} \in \eta$	double line	double line $\neq L$ through $\mathbf{p}$	parabolic cylinder
11	tangent plane	$\mathbf{z} \in \eta$	$\mathbf{s} \in \eta$	double line t	double line L	parabolic cylinder

TABLE 2. Degenerate quadric

The first problem on the way of determining Q's principal axes directions thus consists in answering the question of how to obtain the intersection points $\mathbf{a}, \bar{\mathbf{a}}$ and $\mathbf{b}, \bar{\mathbf{b}}$ of the conics k_η and k_a in the plane at infinity. All we have in order to solve this task is Q's rational quadratic parameter representation (2.1), i.e., the quadric's stereographic projection. We wish to intersect k_η, the quadric's conic at infinity ($k_\eta = Q \cap \eta$) and k_a, the absolute conic which may be obtained by intersecting the minimal cone

$$C_M : x_1^2 + x_2^2 + x_3^2 = 0 \tag{3.2}$$

with the plane at infinity

$$\eta : x_0 = 0,$$

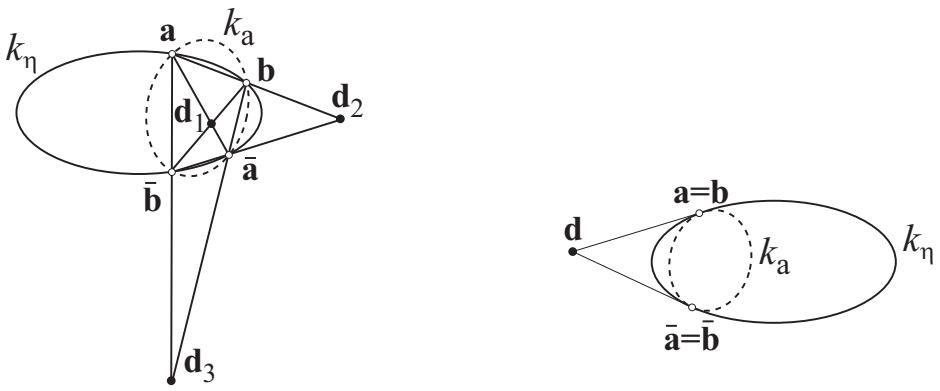

FIGURE 1. Situation in the plane at infinity. Left: general case, $\Delta \mathbf{d}_1\mathbf{d}_2\mathbf{d}_3$ is the common polar triangle of k_η and k_a. Right: case of a quadric of revolution.

i.e., $k_a = C_M \cap \eta$. Let γ be the intersection of the minimal cone C_M and the quadric Q ($\gamma = C_M \cap Q$), thus being an algebraic space curve of order four. It then holds

$$k_a \cap k_\eta = \gamma \cap \eta = \gamma \cap k_\eta. \tag{3.3}$$

We know the stereographic projections

$$\sigma(k_\eta) : x_0(u, v, w) = 0,$$

and

$$\sigma(\gamma) : x_1^2(u, v, w) + x_2^2(u, v, w) + x_3^2(u, v, w) = 0, \tag{3.4}$$

where $\sigma(k_\eta)$ is a conic section in the uvw–plane ϵ, and $\sigma(\gamma)$ is an algebraic curve of order four in ϵ. By Bézout's theorem the intersection of $\sigma(\gamma)$ and $\sigma(k_\eta)$ thus consists of eight points, algebraically counted, whereas the desired intersection $k_a \cap k_\eta$ only consists of four points, algebraically counted. In order to solve this discrepancy we consider the following. The fourth order algebraic space curve γ intersects the tangent plane $T_{\mathbf{z}}$ of Q in the center $\mathbf{z}$ of the stereographic projection in four points. The stereographic projection of these four points yield the degeneration or base points $\mathbf{p}_1, \mathbf{p}_2$ of the quadric[1], the quadric's base points are therefore contained in $\sigma(\gamma)$ as well as in $\sigma(k_\eta)$ thus being part of the intersection $\sigma(\gamma) \cap \sigma(k_\eta)$, and in general counting with multiplicity four.

This yields

$$\sigma(\gamma) \cap \sigma(k_\eta) = \{\mathbf{p}_1, \mathbf{p}_2, \sigma(\mathbf{a}), \sigma(\bar{\mathbf{a}}), \sigma(\mathbf{b}), \sigma(\bar{\mathbf{b}})\}. \tag{3.5}$$

On this basis we may now proceed to practically determine $\sigma(\mathbf{a}), \sigma(\bar{\mathbf{a}}), \sigma(\mathbf{b}), \sigma(\bar{\mathbf{b}})$, and from this $\mathbf{a}, \bar{\mathbf{a}}, \mathbf{b}, \bar{\mathbf{b}}$, and thus $\mathbf{d}_1$, $\mathbf{d}_2$, $\mathbf{d}_3$.

[1]For a degenerate quadric $\mathbf{p}_1 = \mathbf{p}_2$, see page 65.

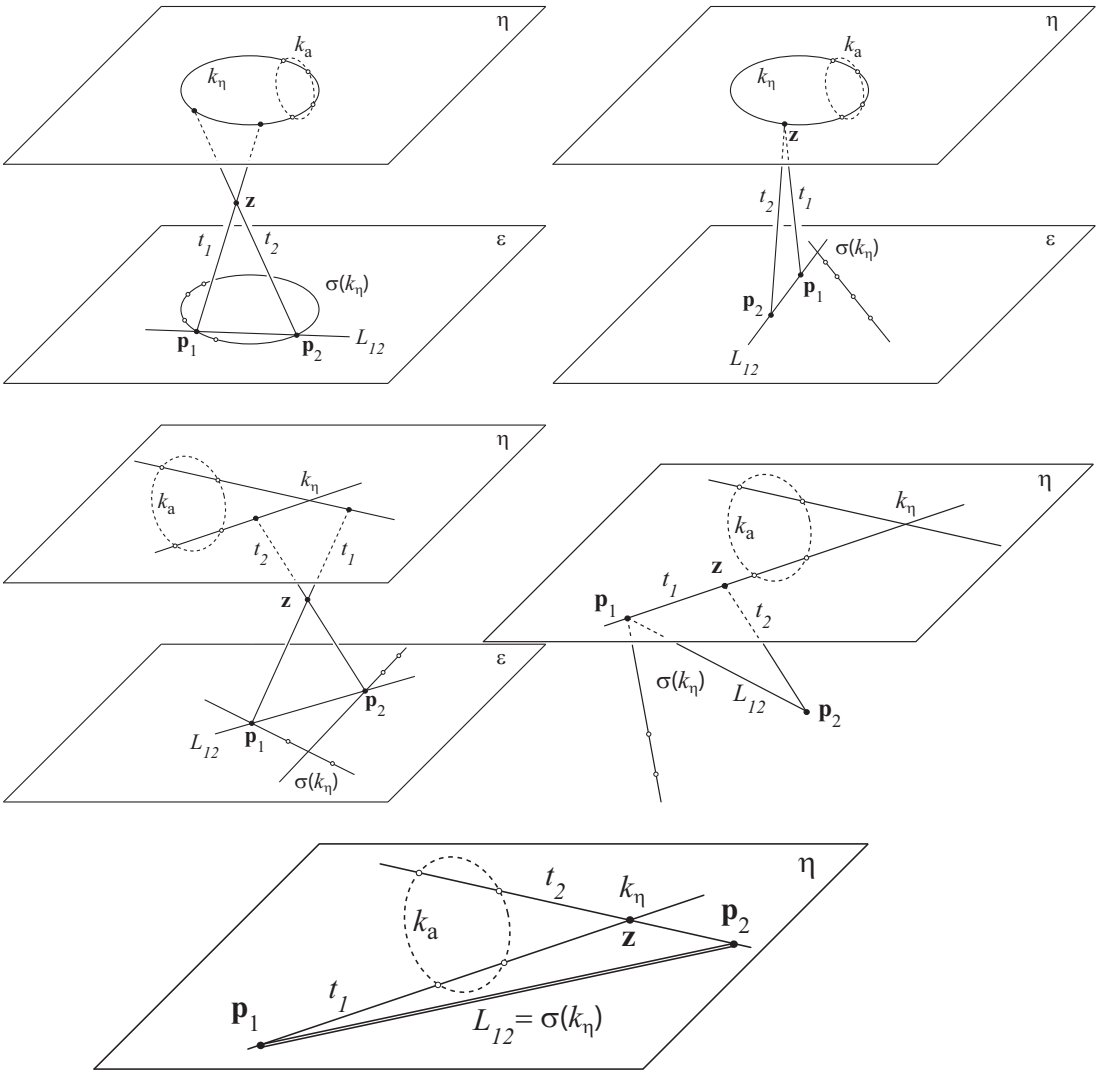

FIGURE 2. Schematic illustration of cases 1–5 from Table 1. First row left: case 1, first row, right: case 2, second row, left: case 3, second row, right: case 4, third row: case 5.

3.2. **Practical determination of the axes directions.** We will now treat the different configurations induced by the 11 cases of tables 1 and 2. They are schematized in Figures 2 and 3 for general quadrics. The situation for quadrics of revolution differs only in the plane at infinity according to Figure 1, right. The four desired points $\sigma(\mathbf{a}), \sigma(\bar{\mathbf{a}}), \sigma(\mathbf{b}), \sigma(\bar{\mathbf{b}}) \in \epsilon$ and their respective preimages $\mathbf{a}, \bar{\mathbf{a}}, \mathbf{b}, \bar{\mathbf{b}} \in \eta$ are marked by hollow circles.

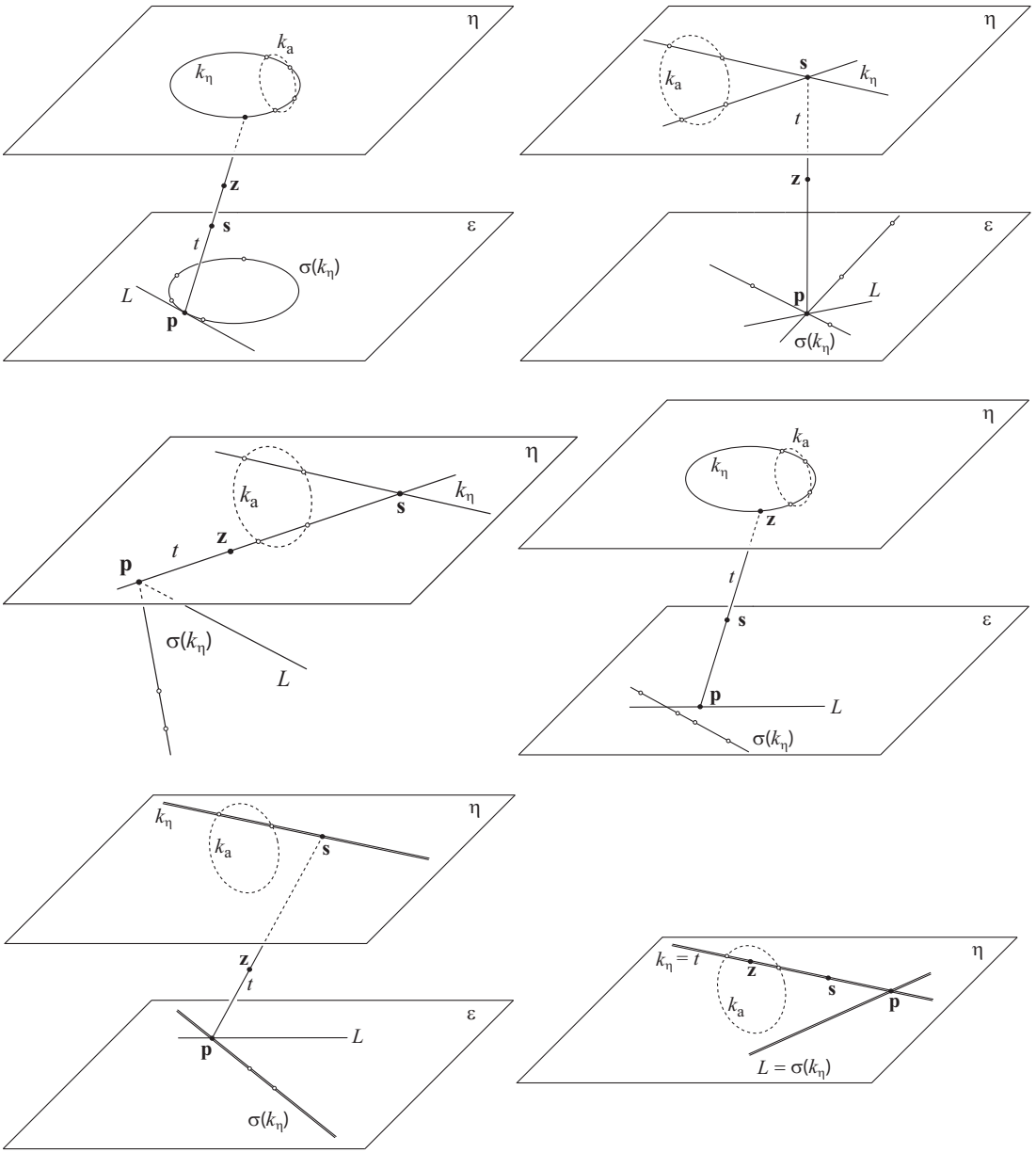

FIGURE 3. Schematic illustration of cases 6–11 from Table 2. First row left: case 6, first row, right: case 7, second row, left: case 8, second row, right: case 9, third row, left: case 10, third row, right: case 11.

In order to practically determine the points $\sigma(\mathbf{a}), \sigma(\bar{\mathbf{a}}), \sigma(\mathbf{b}), \sigma(\bar{\mathbf{b}})$ we first calculate the two base points $\mathbf{p}_i(u_i, v_i, w_i)$, $i = 1, 2$ by solving[2]

$$x_0(u, v, w) = x_1(u, v, w) = x_2(u, v, w) = x_3(u, v, w) = 0.$$

[2]These solutions always exist due to the special geometry of rational quadratic parametrisations of quadrics, see, e.g., [21].

By considering the fact that these base points count with multiplicity four in the intersection of $\sigma(k_\eta)$ and $\sigma(\gamma)$ (see section 3.1), in general, we thus obtain four additional solutions (u_i, v_i, w_i), $i = 3, 4, 5, 6$, which yield the coordinates

$$(x_1(u_i, v_i, w_i), x_2(u_i, v_i, w_i), x_3(u_i, v_i, w_i)) \tag{3.6}$$

of the desired intersection points $\mathbf{a}, \bar{\mathbf{a}}, \mathbf{b}, \bar{\mathbf{b}}$ of k_η and γ in the plane at infinity $x_0 = 0$.

In the exceptional situation that part of the intersection points between k_a and k_η lie in the quadric's tangent plane in $\mathbf{z}$, the multiplicity of the base points on the intersection $\sigma(\gamma) \cap \sigma(k_\eta)$ is higher than four, and in this case we cannot obtain the coordinates of $\mathbf{a}, \bar{\mathbf{a}}, \mathbf{b}, \bar{\mathbf{b}}$ as described above. This latter exceptional situation happens only in the following very special settings (see tables 1,2 and figures 2, 3):

(i) cases 4 and 5, i.e., if Q is a paraboloid and $\mathbf{z} \in \eta$ [3]
(ii) case 1, if $k_a \cap k_\eta \cap T_{\mathbf{z}} \neq \emptyset$; this is possible only if Q is an ellipsoid since $k_a \cap k_\eta$ consists of imaginary points.
(iii) case 3, if $k_a \cap k_\eta \cap T_{\mathbf{z}} \neq \emptyset$; this is possible only if Q is an elliptic paraboloid.
(iv) case 8, i.e., if Q is a hyperbolic cylinder and $\mathbf{z} \in \eta$.
(v) case 11, i.e., if Q is a parabolic cylinder and $\mathbf{z} \in \eta$.

These exceptional cases, where, algebraically speaking, the multiplicity of the quadric's base points in the intersection $\sigma(\gamma) \cap \sigma(k_\eta)$ is higher than four, may easily be reduced to one of the general cases (multiplicity of quadric's base points in $\sigma(\gamma) \cap \sigma(k_\eta)$ is equal to four), by considering another surface patch on the same quadric Q obtained with respect to a different stereographic projection center $\mathbf{z}'$.

In the exceptional situations (i), (iv), (v), i.e., in the cases 4, 5, 8 and 11, we may, e.g., choose (by using (2.1))

$$\mathbf{z}' = \mathbf{x}(\frac{1}{3}, \frac{1}{3}, \frac{1}{3}) \tag{3.7}$$

as finite projection center, since we suppose the triangular patch not to contain poles within the parameter domain $0 \leq u, v, w \leq 1$, $u + v + w = 1$.

In the exceptional situations (ii) and (iii) of cases 1 and 3 we encounter a problem in the case where the center $\mathbf{z}$ of the stereographic projection lies on one of eight specific (complex) lines on the quadric, which are the intersection lines of the tangent planes in the four points $k_a \cap k_\eta$ with the quadric. There exist two families of (complex) lines on the quadric, i.e., a "double" infinity of lines, making these exceptional situations extremely rare! In order to be sure to avoid this very rare setting we consider a parameter curve on the quadric, e.g., the conic $\mathbf{x}(\frac{1}{3}, v, \frac{2}{3} - v)$, which intersects each of the eight lines exactly once. As long as necessary we iteratively generate $v_i = v_{i-1} + \Delta v$, $(i = 1, 2, 3, \ldots)$ and thus $\mathbf{z}'_i = \mathbf{x}(\frac{1}{3}, v_i, \frac{2}{3} - v_i)$, $(i = 0, 1, 2, 3, \ldots)$ for a certain starting value v_0, e.g., $v_0 = \frac{1}{3}$, and a chosen step size Δv. In the worst case (if $\mathbf{z}'_i$ for $i = 0, 1, \ldots, 7$ have not generated a non–exceptional patch) $\mathbf{z}'_8$ guarantees the parametrisation to be non–exceptional. But in practice, should the already very unlikely exceptional setting occur where $\mathbf{z}$ lies on one of the above eight lines, then the first iteration step should remedy.

Once the new projection center $\mathbf{z}'$ has been chosen we generate a new patch on the quadric having the same border points $\mathbf{b}_{200}$, $\mathbf{b}_{020}$, $\mathbf{b}_{002}$ and border weights, but different interior control points and different interior weights. For simplicity we consider a patch in standard form (corner weights =1) and denote the corner

[3] Algebraically this is the case if the paraboloid is given by a polynomial parametrisation, i.e., $x_0(u, v, w) = 1$.

points $\mathbf{b}_{200}$, $\mathbf{b}_{020}$, and $\mathbf{b}_{002}$ by $\mathbf{b}_0^C$, $\mathbf{b}_1^C$, and $\mathbf{b}_2^C$ respectively. Let τ_i be the tangent plane of the quadric in $\mathbf{b}_i^C$ and $e_0 = \tau_1 \cap \tau_2$, $e_1 = \tau_0 \cap \tau_2$, $e_2 = \tau_0 \cap \tau_1$ the respective intersection lines. We then consider the planes

$$\begin{aligned} \epsilon_0 &= plane(\mathbf{z}', \mathbf{b}_1^C, \mathbf{b}_2^C) \\ \epsilon_1 &= plane(\mathbf{z}', \mathbf{b}_0^C, \mathbf{b}_2^C) \\ \epsilon_2 &= plane(\mathbf{z}', \mathbf{b}_0^C, \mathbf{b}_1^C) \end{aligned}$$

generated by the new projection center and a pair of corner points. The new interior control point $\mathbf{b}_i'^I \in e_i$ $(i = 0, 1, 2)$ is then obtained as intersection of the plane ϵ_i and the line e_i ($\mathbf{b}_i'^I \epsilon_i \cap \in e_i$) calculated as solution of a 3×3 linear equation system. According to [20] the weight $w_i'^I$ (which can become negative) in the point $\mathbf{b}_i'^I$ is calculated from

$$w_i'^I (\mathbf{b}_i'^I - \mathbf{z}') = \mathbf{q}_i - \mathbf{z}' \,, \tag{3.8}$$

where

$$\begin{aligned} \mathbf{q}_0 &= \mathbf{z}'\mathbf{b}_0'^I \cap \mathbf{b}_1^C \mathbf{b}_2^C \,, \\ \mathbf{q}_1 &= \mathbf{z}'\mathbf{b}_1'^I \cap \mathbf{b}_0^C \mathbf{b}_2^C \,, \\ \mathbf{q}_2 &= \mathbf{z}'\mathbf{b}_2'^I \cap \mathbf{b}_0^C \mathbf{b}_1^C \,. \end{aligned}$$

Remark 3.1. The calculations of the new interior control points and weights may be avoided in the situations (i), (iv) and (v) if the intersection point $\mathbf{p}$ of the tangent planes τ_i ($\mathbf{p} = \tau_0 \cap \tau_1 \cap \tau_2$) does not lie in the plane at infinity η. Let $\mathbf{e}_i$ denote the intersection points of the line e_i and the plane π generated by the corner points of the patch, and let $\mathbf{b}_i^I = \lambda_i \mathbf{p} + \mu_i \mathbf{e}_i$ be the old interior control points $(i = 0, 1, 2)$. Then, according to [5, 6] the so–called harmonic complement of the given quadric patch is obtained by using as new interior control points

$$\mathbf{b}_i'^I = -\lambda_i \mathbf{p} + \mu_i \mathbf{e}_i$$

and corresponding weights. This choice guarantees the associated stereographic projection center $\mathbf{z}'$ not to lie in the plane at infinity η (supposing that $\mathbf{z} \in \eta$ and $\mathbf{p} \notin \eta$). This is due to the fact that the points $\mathbf{p}$, $\mathbf{z}$, and $\mathbf{z}'$ are colinear. This may be shown by appropriately combining the constructions from [6] and [20]. Furthermore the points $(\mathbf{z}', \mathbf{z}, \mathbf{p}, \mathbf{s})$, where $\mathbf{s} = \mathbf{pz} \cap \pi$, inherit the harmonic position from the harmonic position of the points $(\mathbf{b}_i'^I, \mathbf{b}_i^I, \mathbf{p}, \mathbf{e}_i)$, $(i = 0, 1, 2)$.

We may thus suppose our configuration to be such that of the eight intersection points $\sigma(\gamma) \cap \sigma(k_\eta)$, algebraically counted, four are the base points of Q, and the remaining four are the stereographic projections of the desired points $\mathbf{a}, \bar{\mathbf{a}}, \mathbf{b}, \bar{\mathbf{b}}$. Once we have calculated the (u, v, w)–values of $\sigma(\mathbf{a}), \sigma(\bar{\mathbf{a}}), \sigma(\mathbf{b}), \sigma(\bar{\mathbf{b}})$ we then substitute them into the numerator of the quadric's parameter representation and obtain the coordinates (3.6) of the four points $\mathbf{a}, \bar{\mathbf{a}}, \mathbf{b}, \bar{\mathbf{b}}$ in the plane at infinity.

We distinguish the following cases:

Case 1: $\mathbf{a} \neq \mathbf{b}$ (see figure 1, left)

In this case we have two pairs of conjugate complex points $(\mathbf{a}, \bar{\mathbf{a}})$ and $(\mathbf{b}, \bar{\mathbf{b}})$ which form a non-degenerate quadrilateral in the plane at infinity. We then calculate the intersection points $\mathbf{d}_1, \mathbf{d}_2, \mathbf{d}_3$ of the diagonals of this quadrilateral $\mathbf{a}, \bar{\mathbf{a}}, \mathbf{b}, \bar{\mathbf{b}}$, and thus know the directions of Q's principal axes. Practically, this may be accomplished in the following way. The connecting

line of the two points $\mathbf{p}(p_1, p_2, p_3)$ and $\mathbf{q}(q_1, q_2, q_3)$ in the plane at infinity (i.e., $p_0 = q_0 = 0$) has the representation

$$l_{\mathbf{pq}}: \quad \mathbf{l_{pq}} \cdot \mathbf{x} = 0, \quad x_0 = 0, \tag{3.9}$$

where $\mathbf{x} = (x_1, x_2, x_3)$ and $\mathbf{l_{pq}} = \mathbf{p} \wedge \mathbf{q}$ ("$\wedge$" stands for the vector product). In this way we determine the six lines $l_{\mathbf{a\bar{a}}}$, $l_{\mathbf{b\bar{b}}}$, $l_{\mathbf{ab}}$, $l_{\mathbf{\bar{a}\bar{b}}}$, $l_{\mathbf{a\bar{b}}}$, $l_{\mathbf{\bar{a}b}}$, and the intersection points of the three pairs of opposite diagonals as

$$\mathbf{d}_1 = \mathbf{l_{a\bar{a}}} \wedge \mathbf{l_{b\bar{b}}}\,, \ \mathbf{d}_2 = \mathbf{l_{ab}} \wedge \mathbf{l_{\bar{a}\bar{b}}}\,, \ \mathbf{d}_3 = \mathbf{l_{a\bar{b}}} \wedge \mathbf{l_{\bar{a}b}}\,. \tag{3.10}$$

An interesting side product of these considerations is the following. Since circles are exactly those conics containing two points of the absolute conic k_a all the planes containing any two of the points $\mathbf{a}, \bar{\mathbf{a}}, \mathbf{b}, \bar{\mathbf{b}}$ are candidates for carrying circular sections of the quadric Q, but only those containing $(\mathbf{a}, \bar{\mathbf{a}})$ respectively $(\mathbf{b}, \bar{\mathbf{b}})$ yield real circles. We thus have

Proposition 3.1. *If the quadric Q is an ellipsoid, a hyperboloid of one sheet, a hyperboloid of two sheets, an elliptic paraboloid, a cone or an elliptic cylinder the two systems of parallel planes yielding circular sections of Q are given by all the planes having either $l_{\mathbf{a\bar{a}}}$ or $l_{\mathbf{b\bar{b}}}$ as line at infinity.*

Case 2: $\mathbf{a} = \mathbf{b}$ and k_η is not a double line (see figure 1, right)

We are in the case of a quadric of revolution, and we have one pair of conjugate complex points $(\mathbf{a}, \bar{\mathbf{a}})$ in the plane at infinity. In this case there exists only one system of parallel planes yielding circular sections on Q, namely the planes that are perpendicular to the direction of the axis of rotation. They all contain the points $\mathbf{a}$ and $\bar{\mathbf{a}}$ in the plane at infinity, and thus satisfy an equation of the form

$$\lambda x_0 + \mathbf{l_{a\bar{a}}} \cdot \mathbf{x} = 0\,, \ \lambda \in \mathbb{R}$$

where $\mathbf{x} = (x_1, x_2, x_3)$ and $\mathbf{l_{a\bar{a}}} = \mathbf{a} \wedge \bar{\mathbf{a}}$. $\mathbf{l_{a\bar{a}}}$ thus provides the direction of Q's axis of rotation. The remaining two directions may be chosen as arbitrary orthogonal directions within the plane $\mathbf{l_{a\bar{a}}} \cdot \mathbf{x} = 0$.

Case 3: $\mathbf{a} = \mathbf{b}$ and k_η is a double line (case 10)

We are in the case of a parabolic cylinder, and we have one pair of conjugate complex points $(\mathbf{a}, \bar{\mathbf{a}})$ in the plane at infinity. An arbitrary plane through the line k_η is given by

$$\pi_\lambda: \quad \lambda x_0 + \mathbf{l_{a\bar{a}}} \cdot \mathbf{x} = 0 \ \text{ for } \lambda \in \mathbb{R}, \tag{3.11}$$

where $\mathbf{x} = (x_1, x_2, x_3)$ and $\mathbf{l_{a\bar{a}}} = \mathbf{a} \wedge \bar{\mathbf{a}}$. The planes π_λ are parallel planes all having the same normal vector $\mathbf{l_{a\bar{a}}}$, which thus yields one of the desired axis directions, $\mathbf{d}_1 = \mathbf{l_{a\bar{a}}}$. The intersection line $\pi_\lambda \cap Q$ yields a generating line of Q and thus another axis direction. Practically, we may obtain this axis direction by inserting Q's parameter representation into π_λ's implicit equation (3.11), and thus obtaining a second order equation of the form

$$f_\lambda(u, v, w) = l(u, v, w) \cdot m_\lambda(u, v, w) = 0,$$

where $l(u, v, w)$, $m_\lambda(u, v, w)$ are linear factors representing the stereographic projections of the parabolic cylinders' line at infinity ($l(u, v, w) = 0$) and one proper generating line ($m_\lambda(u, v, w) = 0$), respectively. We thus map two of the points of $m_\lambda(u, v, w) = 0$ back onto Q obtaining $\mathbf{p}_\lambda, \mathbf{q}_\lambda \in Q$, and

their connecting vector $\mathbf{d}_2 = \mathbf{p}_\lambda - \mathbf{q}_\lambda$ yields the desired axis direction. The remaining axis direction $\mathbf{d}_3$ is thus obtained as $\mathbf{d}_3 = \mathbf{d}_1 \wedge \mathbf{d}_2$.[4]

Case 4: $k_\eta = k_a$

In this case the quadric Q is a sphere and no intersection points $\mathbf{a}, \bar{\mathbf{a}}, \mathbf{b}, \bar{\mathbf{b}}$ exist. This case has to be tested upfront. Practically, this may be done by checking if the sum of the squares of the coefficients of Sylvester's resultant of the equations (2.4) and (3.4) is smaller then a given tolerance. In this case three arbitrary pairwise orthogonal directions may be chosen as axes of the sphere Q.

4. Determination of the origin

In order to determine the origin such that the quadric Q is in canonical position with respect to the resulting coordinate system, we will separately consider the class of central quadrics (i.e., ellipsoids, hyperboloids of one and two sheets), the class of paraboloids (i.e., elliptic and hyperbolic paraboloids), and the class of cones and cylinders (i.e., cones, and elliptic, hyperbolic and parabolic cylinders).

4.1. **Central quadrics.** In the case of the central quadrics the desired origin $\mathbf{o}$ coincides with the center of the quadric, and it may be obtained as the intersection of the quadric's symmetry planes. Since we already know the axes directions of the quadric Q, it is sufficient to determine one quadric point in each symmetry plane in order to analytically obtain these planes. Let π_i be the symmetry plane of Q that is orthogonal to the axis direction $\mathbf{d}_i$, and let c_i be the intersection curve of π_i and Q ($c_i = \pi_i \cap Q$). c_i is a conic section, the so–called silhouette conic of Q with respect to the direction $\mathbf{d}_i$, and it is characterized by the fact that Q's normals along c_i are perpendicular to $\mathbf{d}_i$. If we write the parameter representation (2.1) as

$$\mathbf{x}(u, v, w) = \frac{\mathbf{p}(u, v)}{\rho(u, v)},$$

where $w = 1 - u - v$, then Q's normal vector is parallel to

$$\mathbf{n}(u, v) = \rho(u, v)\mathbf{p}_u(u, v) \wedge \mathbf{p}_v(u, v) - \rho_v(u, v)\mathbf{p}_u(u, v) \wedge \mathbf{p}(u, v) - \rho_u(u, v)\mathbf{p}(u, v) \wedge \mathbf{p}_v(u, v)\,,$$

where $\mathbf{p}_u(u, v)$, $\mathbf{p}_v(u, v)$ respectively $\rho_u(u, v)$, $\rho_v(u, v)$denote $\mathbf{p}$'s respectively ρ's partial derivatives. It turns out that the components of $\mathbf{n}(u, v)$ are cubic polynomials on (u, v). In the (u, v)–parameter plane ϵ the silhouette conic c_i is thus characterized by the cubic equation

$$\mathbf{d}_i \cdot \mathbf{n}(u, v) = 0. \tag{4.1}$$

c_i's stereographic projection $\sigma(c_i)$ is either a straight line or a conic section in ϵ depending on whether the projection center $\mathbf{z}$ lies on c_i ($\mathbf{z} \in c_i$) or not ($\mathbf{z} \notin c_i$). The cubic equation (4.1) decomposes into a quadratic component for $\sigma(c_i)$ and a linear one for the base line, and if $\mathbf{z} \in c_i$ equation (4.1) factorizes into the doubly counting base line and linear component describing the line $\sigma(c_i)$.

All we need for our purpose of determining the quadric's symmetry planes is one point on c_i. We may obtain such a point by intersecting an arbitrary line in ϵ with the cubic curve (4.1). Of the three resulting intersection points we choose one that is not contained in the quadric's base line and calculate its image point on

[4]This line of reasoning even permits to determine the position of the origin $\mathbf{p}_\lambda$ with λ satisfying $\mathbf{n}_\lambda \cdot \mathbf{l}_{\mathbf{a}\bar{\mathbf{a}}} = 0$, where $\mathbf{n}_\lambda$ is a normal vector of Q in $\mathbf{p}_\lambda$.

the quadric by using the parameter representation (2.1). Together with the known axes directions this yields the three symmetry planes of the central quadric Q and their intersection point is the desired origin $\mathbf{o}$. With respect to $\{\mathbf{o}; \mathbf{d}_1, \mathbf{d}_2, \mathbf{d}_3\}$ the quadric Q from (2.1) has canonical form.

4.2. **Paraboloids, cones and cylinders.** In the case of a paraboloid, a cone or a cylinder two of the symmetry planes may be obtained in the same way as for central quadrics, see section 4.1. The only difference consists in the fact that, here, in some cases the base line might lie in the plane at infinity. If this is the case, equation (4.1) is of degree two, and directly describes $\sigma(c_i)$.

The intersection of the two symmetry planes yields one axis of the quadric, say d_1. If Q is a paraboloid or a cone we then intersect d_1 with Q and obtain the desired origin $\mathbf{o}$. If Q is a cylinder we arbitrarily choose the origin $\mathbf{o}$ on d_1. The remaining two axes d_2, d_3 are then obtained by simply attaching the already known remaining two axes' directions $\mathbf{d}_2, \mathbf{d}_3$ in the origin $\mathbf{o}$. Thus the quadric Q has canonical form with respect to the coordinate system $\{\mathbf{o}; \mathbf{d}_1, \mathbf{d}_2, \mathbf{d}_3\}$.

5. Examples

In this section we illustrate the method of determining the coordinate system with respect to which the quadric carrying the given triangular parametric quadric patch has canonical position. The presented algorithm has been implemented in the computer algebra system Maple, whose procedures are used for the performed tasks such as equation solving, and has been tested for numerous examples. The most significant ones, illustrating the main aspects of the method are listed below. The figures have been produced with the program Geomview.

Without loss of generality we suppose the rational triangular quadric patch to be given in standard form (i.e., $w_{002} = w_{020} = w_{200} = 1$). For every example we thus give the control points and the inner weights as input data. As a result of the algorithm detailed in [3] we first obtain the affine type of the underlying quadric. On this basis we then apply the algorithm explained in the previous sections and display and interpret the numerical results for the

- base points,
- intersection points $\sigma(k_\eta) \cap \sigma(\gamma)$,
- points $\mathbf{a}, \bar{\mathbf{a}}, \mathbf{b}, \bar{\mathbf{b}}$ in the plane at infinity,
- axis directions $\mathbf{d}_1, \mathbf{d}_2, \mathbf{d}_3$,
- curves $\mathbf{d}_i \cdot \mathbf{n}(u, v) = 0$ (see (4.1)),
- origin.

In order to verify the numerical results, in the following examples we use, without loss of generality, triangular parametric patches on quadrics that are in canonical position with respect to the given coordinate system. The algorithm thus has to yield this original coordinate system $\{\mathbf{o}(0,0,0); (1,0,0)^T, (0,1,0)^T, (0,0,1)^T\}$ as result.

The below examples have been calculated with a 10–digit numerical accuracy.

Example 1 Input:

$$\begin{aligned}
\mathbf{b}_{002} &= (-.9171974522, -.9171974522, -.8343949045)^T,\\
\mathbf{b}_{020} &= (0, 1.6, -.6)^T,\\
\mathbf{b}_{200} &= (1.704142012, -.8520710059, -.7041420118)^T,\\
\mathbf{b}_{011} &= (-.5714285715, .5714285715, -1.285714286)^T,\\
\mathbf{b}_{101} &= (.4965517242, -.9931034485, -.9862068965)^T,\\
\mathbf{b}_{110} &= (1.142857143, .5714285715, -1.285714286)^T,
\end{aligned}$$

$$w_{011} = .7495221408,\ w_{101} = .8901738325,\ w_{110} = .7224219618.$$

The algorithm from [3] yields case 1 (see table 1), the patch thus lies on an **ellipsoid**, see Figure 4, left.

Output: – base points:

$$\begin{aligned}
(u_1, v_1) &= (10.28131051 - 16.78776028 \cdot I, 9.508813267 + 9.186826300 \cdot I),\\
(u_2, v_2) &= (10.28131056 + 16.78776033 \cdot I, 9.508813267 - 9.186826300 \cdot I).
\end{aligned}$$

– additional intersection points of $\sigma(k_\eta)$ and $\sigma(\gamma)$:

$$\begin{aligned}
(u_3, v_3) &= (-1.459354858 - .4517579514 \cdot I, .5479983730 + 1.799168251 \cdot I),\\
(u_4, v_4) &= (1.624652414 - .6814995422 \cdot I, .4728876873 + 1.614092433 \cdot I),\\
(u_5, v_5) &= (1.624652414 + .6814995422 \cdot I, .4728876873 - 1.614092433 \cdot I),\\
(u_6, v_6) &= (-1.459354858 + .4517579514 \cdot I, .5479983730 - 1.799168251 \cdot I),
\end{aligned}$$

– points $\mathbf{a}$ and $\mathbf{b}$ yielding the quadrilateral $\mathbf{a}\bar{\mathbf{a}}\mathbf{b}\bar{\mathbf{b}}$ in the plane at infinity:

$$\mathbf{a} = \begin{pmatrix} -4.360263687 + .8886790196 \cdot I \\ .967471190 + 4.746853823 \cdot I \\ -1.876358720 + .382426572 \cdot I \end{pmatrix},$$

$$\mathbf{b} = \begin{pmatrix} 3.501421523 + .6362208299 \cdot I \\ .692629498 - 3.811864965 \cdot I \\ -1.506771938 - .273785841 \cdot I \end{pmatrix}.$$

– axes directions $\mathbf{d}_1, \mathbf{d}_2, \mathbf{d}_3$:

$$\begin{aligned}
\mathbf{d}_1 &= (.8378892704 \cdot 10^{-8}, -1., .4917694781 \cdot 10^{-9})^T,\\
\mathbf{d}_2 &= (.1482689201 \cdot 10^{-7}, -.1680085742 \cdot 10^{-9},\\
&\quad .9999999998)^T,\\
\mathbf{d}_3 &= (-.9999999996, -.5151280985 \cdot 10^{-8},\\
&\quad .1652759080 \cdot 10^{-8})^T
\end{aligned}$$

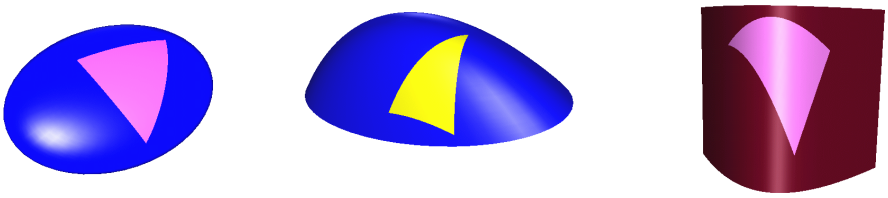

FIGURE 4. Illustration of the given quadric triangles together with their underlying quadrics for the examples 1 (left), 2 (middle), and 3 (right).

– curves $\mathbf{d}_i \cdot \mathbf{n}(u,v) = 0$ (see (4.1)):

$$\begin{aligned}
\mathbf{d}_1 \cdot \mathbf{n}(u,v) &= .7386800406 \cdot 10^{-4} \cdot u^3 + .6128967978 \cdot 10^{-2} \cdot u^2 \cdot v \\
&\quad +.2165985099 \cdot 10^{-1} \cdot u \cdot v^2 + .1956493578 \cdot 10^{-1} \cdot v^3 \\
&\quad -.6128971499 \cdot 10^{-2} \cdot u^2 - .3390236733 \cdot u \cdot v \\
&\quad -.5990563440 \cdot v^2 + .1695118177 \cdot u \\
&\quad +4.688267021 \cdot v - 1.562755669 \\
&= 0, \\
\mathbf{d}_2 \cdot \mathbf{n}(u,v) &= .5353578295 \cdot 10^{-1} \cdot u^3 + .1364407931 \cdot u^2 \cdot v \\
&\quad +.1920287660 \cdot u \cdot v^2 + .2219749983 \cdot v^3 \\
&\quad -1.502102728 \cdot u^2 - 1.170769792 \cdot u \cdot v \\
&\quad -3.476038635 \cdot v^2 + .3873330520 \cdot u \\
&\quad +1.386399279 \cdot v + 5.686694271 \\
&= 0, \\
\mathbf{d}_3 \cdot \mathbf{n}(u,v) &= .2658327937 \cdot 10^{-2} \cdot u^3 + .1062351426 \cdot 10^{-1} \cdot u^2 \cdot v \\
&\quad +.1219543143 \cdot 10^{-1} \cdot u \cdot v^2 + .3032066467 \cdot 10^{-2} \cdot v^3 \\
&\quad -.1479532018 \cdot u^2 - .3222507015 \cdot u \cdot v \\
&\quad -.9481322440 \cdot 10^{-1} \cdot v^2 + 2.083674235 \cdot u \\
&\quad +.7863392582 \cdot v - .6945580770 \\
&= 0.
\end{aligned}$$

– origin (obtained as intersection of the three symmetry planes): $\mathbf{o}(-.2365961050 \cdot 10^{-7}, .3063806432 \cdot 10^{-8}, -.1208053726 \cdot 10^{-7})$.

Example 2 Input:

$$\begin{aligned}
\mathbf{b}_{002} &= (1,1,1.25)^T,\\
\mathbf{b}_{020} &= (0,1,1)^T,\\
\mathbf{b}_{200} &= (1,0,.25)^T,\\
\mathbf{b}_{011} &= (.5,1,1)^T,\\
\mathbf{b}_{101} &= (1,.5,.25)^T,\\
\mathbf{b}_{110} &= (.5,.5,0)^T,
\end{aligned}$$

$$w_{011} = 1,\ w_{101} = 1,\ w_{110} = 1.$$

The algorithm from [3] yields case 5 (see table 1), the patch thus lies on an **elliptic paraboloid**, see Figure 4, middle.
According to the listing of exceptional cases, see section 3.2, and figure 2, bottom, the given parametrisation is not suitable for the calculations. We therefore construct the harmonic complement of the given patch and thus obtain the following — suitable — input data (we are now in case 3):

$$\begin{aligned}
\mathbf{b}_{002} &= (1,1,1.25)^T,\\
\mathbf{b}_{020} &= (0,1,1)^T,\\
\mathbf{b}_{200} &= (1,0,.25)^T,\\
\mathbf{b}_{011} &= (1/2,4/3,5/3)^T,\\
\mathbf{b}_{101} &= (-1/3,1/2,-5/12)^T,\\
\mathbf{b}_{110} &= (1/2,1/2,0)^T,
\end{aligned}$$

$$w_{011} = 3/5,\ w_{101} = -3/5,\ w_{110} = -1.$$

Output:

– base points:

$$\begin{aligned}
(u_1,v_1,w_1) &= (1/2\cdot I,1,0),\\
(u_2,v_2,w_2) &= (-.5000000000\cdot I,1,0).
\end{aligned}$$

– additional intersection points of $\sigma(k_\eta)$ and $\sigma(\gamma)$:

$$\begin{aligned}
(u_3,v_3) &= (.6106759983 + .2025512905\cdot 10^{-1}\cdot I, .5405102585 - .2213519966\cdot I),\\
(u_4,v_4) &= (.2089116900 - .1988170358\cdot I, .8976340716 - .5821766201\cdot I),\\
(u_5,v_5) &= (.2089116900 + .1988170358\cdot I, .8976340716 + .5821766201\cdot I),\\
(u_6,v_6) &= (.6106759983 - .2025512905\cdot 10^{-1}\cdot I, .5405102585 + .2213519966\cdot I),
\end{aligned}$$

– points $\mathbf{a}$ and $\mathbf{b}$ yielding the quadrilateral $\mathbf{a\bar{a}b\bar{b}}$ in the plane at infinity:

$$\mathbf{a} = \begin{pmatrix} -.4051025852\cdot 10^{-1} + .2213519966\cdot I \\ -.1106759983 - .2025512904\cdot 10^{-1}\cdot I \\ .1916964369 + .3508287013\cdot 10^{-1}\cdot I \end{pmatrix},$$

$$\mathbf{b} = \begin{pmatrix} -.3976340716 - .5821766201\cdot I \\ .2910883100 - .1988170357\cdot I \\ .5041797921 - .3443611905\cdot I \end{pmatrix}.$$

– axes directions $\mathbf{d}_1, \mathbf{d}_2, \mathbf{d}_3$:

$$\begin{aligned}
\mathbf{d}_1 &= (-1., .3292829096 \cdot 10^{-7}, .1163963355 \cdot 10^{-6})^T, \\
\mathbf{d}_2 &= (.1204583774 \cdot 10^{-8}, -.1108513701 \cdot 10^{-10}, \\
&\quad -.9999999996)^T, \\
\mathbf{d}_3 &= (-.1334980598 \cdot 10^{-6}, -1., -.1459103704 \cdot 10^{-6})^T
\end{aligned}$$

– curves $\mathbf{d}_i \cdot \mathbf{n}(u, v) = 0$ (see (4.1)):

$$\begin{aligned}
\mathbf{d}_1 \cdot \mathbf{n}(u,v) &= .8000002671 \cdot u^2 + .2000000668 \cdot v^2 \\
&\quad -.8000002013 \cdot u - .7000000668 \cdot v \\
&\quad +.5000000505 \\
&= 0, \\
\mathbf{d}_3 \cdot \mathbf{n}(u,v) &= 3.199999640 \cdot u^2 + .7999999100 \cdot v^2 \\
&\quad -5.199999640 \cdot u - .7999999767 \cdot v \\
&\quad +1.999999921 \\
&= 0.
\end{aligned}$$

– origin (obtained as intersection of two symmetry planes and the quadric): $\mathbf{o}(-.2165476376 \cdot 10^{-6} - .6754367456 \cdot 10^{-14} \cdot I, .497938674 \cdot 10^{-7} - .2051234632 \cdot 10^{-6} \cdot I, 0. - .2043 \cdot 10^{-13} \cdot I)$.

Example 3 Input:

$$\begin{aligned}
\mathbf{b}_{002} &= (2.312941292, .5808823929, 1.458823657)^T, \\
\mathbf{b}_{020} &= (2.065591118, .2581988897, 2.581988897)^T, \\
\mathbf{b}_{200} &= (2.285714286, -.5532833353, 1.428571429)^T, \\
\mathbf{b}_{011} &= (2.141704770, .4104261923, 2.052130962)^T, \\
\mathbf{b}_{101} &= (1.739889546, .01044203266, .8220994950)^T, \\
\mathbf{b}_{110} &= (1.872983347, -.1270166538, 1.454972244)^T,
\end{aligned}$$

$$w_{011} = 1.011042669,\ w_{101} = 1.149581073,\ w_{110} = 1.077774309.$$

The algorithm from [3] yields case 7 (see table 2), the patch thus lies on a **hyperbolic cylinder**, see Figure 4, right.

Output:

– base point:

$$(u_1, v_1) = (-9.296915348, 35.37584342),$$

– additional intersection points of $\sigma(k_\eta)$ and $\sigma(\gamma)$:

$$\begin{aligned}
(u_2, v_2) &= (-.9372534534 - .5225407490 \cdot I, -2.051323698 + 2.339472807 \cdot I), \\
(u_3, v_3) &= (-.9372534534 + .5225407490 \cdot I, -2.051323698 - 2.339472807 \cdot I), \\
(u_4, v_4) &= (3.281271232 - 10.56535655 \cdot I, -2.680148265 + 31.96604446 \cdot I), \\
(u_5, v_5) &= (3.281271232 + 10.56535655 \cdot I, -2.680148265 - 31.96604446 \cdot I),
\end{aligned}$$

– points $\mathbf{a}$ and $\mathbf{b}$ yielding the quadrilateral $\mathbf{a\bar{a}b\bar{b}}$ in the plane at infinity:

$$\mathbf{a} = \begin{pmatrix} 4.85128819 - .608861218 \cdot I \\ 2.425644097 - .3044306111 \cdot I \\ .680727551 + 5.423905074 \cdot I \end{pmatrix},$$
$$\mathbf{b} = \begin{pmatrix} 1.4474416 - 8.2584412 \cdot I \\ -.7237222804 + 4.129220339 \cdot I \\ 9.2332155 + 1.6182918 \cdot I \end{pmatrix}.$$

– axes directions $\mathbf{d}_1, \mathbf{d}_2, \mathbf{d}_3$:

$$\begin{aligned} \mathbf{d}_1 &= (-.2150449893 \cdot 10^{-6}, -.1078581048 \cdot 10^{-6}, 1.)^T, \\ \mathbf{d}_2 &= (-.2028174164 \cdot 10^{-6}, .9999999996, \\ &\quad .3939173514 \cdot 10^{-6})^T, \\ \mathbf{d}_3 &= (-1., .5587201313 \cdot 10^{-7}, -.7512289131 \cdot 10^{-7})^T \end{aligned}$$

– curves $\mathbf{d}_i \cdot \mathbf{n}(u, v) = 0$ (see (4.1)):

$$\begin{aligned} \mathbf{d}_2 \cdot \mathbf{n}(u,v) &= -.4390547921 \cdot 10^{-2} \cdot u^3 - .4314756521 \cdot 10^{-1} \cdot u^2 \cdot v \\ &\quad -.2560381189 \cdot 10^{-1} \cdot u \cdot v^2 - .3875600924 \cdot 10^{-2} \cdot v^3 \\ &\quad +1.403925307 \cdot u^2 + 1.009232752 \cdot u \cdot v \\ &\quad +.1732714439 \cdot v^2 - 4.799043995 \cdot u \\ &\quad -1.438242762 \cdot v + 2.087569143 \\ &= 0, \\ \mathbf{d}_3 \cdot \mathbf{n}(u,v) &= -.1828907162 \cdot u^3 - .1647954154 \cdot u^2 \cdot v \\ &\quad -.4973728042 \cdot 10^{-1} \cdot u \cdot v^2 - .5055958016 \cdot 10^{-2} \cdot v^3 \\ &\quad +.7288142485 \cdot u^2 + .4548156334 \cdot u \cdot v \\ &\quad +.7417269768 \cdot 10^{-1} \cdot v^2 - 1.269013251 \cdot u \\ &\quad -.5097287993 \cdot v + 2.078055825 \\ &= 0. \end{aligned}$$

– origin (arbitrarily chosen on the intersection line of two symmetry planes for , e.g., $z = 0$):
$\mathbf{o}(.2080359226 \cdot 10^{-6} - .5866136711 \cdot 10^{-6} \cdot I, .8277369062 \cdot 10^{-6} - .1189754692 \cdot 10^{-12} \cdot I, 0)$.

Example 4 Input:

$$\begin{aligned} \mathbf{b}_{002} &= (-.7826086957, -.7826086957, -.5652173913)^T, \\ \mathbf{b}_{020} &= (0., 1., 0.)^T, \\ \mathbf{b}_{200} &= (1.469387755, -.7346938776, -.4693877551)^T, \\ \mathbf{b}_{011} &= (-1., 1., -3.)^T, \\ \mathbf{b}_{101} &= (.4186046512, -.8372093023, -.6744186047)^T, \\ \mathbf{b}_{110} &= (2., 1., -3.)^T, \end{aligned}$$

$$w_{011} = .3127716211,\ w_{101} = .9057148735,\ w_{110} = .3030457634.$$

The algorithm from [3] yields case 1 (see table 1), the patch thus lies on an **ellipsoid**.

Output: – base points:

$$(u_1, v_1) = (3.212386565 - 11.59368285 \cdot I, 4.484963134 + 1.796329422 \cdot I),$$
$$(u_2, v_2) = (3.212386565 + 11.59368285 \cdot I, 4.484963134 - 1.796329422 \cdot I).$$

– additional intersection points of $\sigma(k_\eta)$ and $\sigma(\gamma)$:

$$(u_3, v_3) = (.1755774319 - .2360520294 \cdot I, .4841871165 + .6934756743 \cdot I),$$
$$(u_4, v_4) = (.1755774319 - .2360520294 \cdot I, .4841871165 + .6934756743 \cdot I),$$
$$(u_5, v_5) = (.1755774319 + .2360520294 \cdot I, .4841871165 - .6934756743 \cdot I),$$
$$(u_6, v_6) = (.1755774319 + .2360520294 \cdot I, .4841871165 - .6934756743 \cdot I),$$

– point $\mathbf{a}$ $(= \mathbf{b})$ in the plane at infinity:

$$\mathbf{a} = \begin{pmatrix} .4719652863 \cdot 10^{-15} + .3020407411 \cdot 10^{-14} \cdot I \\ .370348752 + 1.233212378 \cdot I \\ -1.233212378 + .3703487524 \cdot I \end{pmatrix},$$

We are thus in the case of an ellipsoid of revolution.

– direction of the axis of rotation $\mathbf{d}_1$:

$$\mathbf{d}_1 = (-1., .2778123957 \cdot 10^{-29}, -.1589099487 \cdot 10^{-29})^T,$$

and choice of the remaining two axes directions as

$$\mathbf{d}_2 = (0, 1, 1)^T,$$
$$\mathbf{d}_3 = (0, 1, -1)^T,$$

– curves $\mathbf{d}_i \cdot \mathbf{n}(u, v) = 0$ (see (4.1)):

$$\begin{aligned} \mathbf{d}_1 \cdot \mathbf{n}(u,v) &= .1054513601 \cdot 10^{-2} \cdot u^3 + .1397081004 \cdot 10^{-1} \cdot u^2 \cdot v \\ &\quad + .4855948039 \cdot 10^{-1} \cdot u \cdot v^2 + .1495200927 \cdot 10^{-1} \cdot v^3 \\ &\quad - .6818266625 \cdot 10^{-1} \cdot u^2 - .4654606561 \cdot u \cdot v \\ &\quad - .1639545074 \cdot v^2 + 1.113650215 \cdot u \\ &\quad + .5202192367 \cdot v - .3712167385 \\ &= 0, \\ \mathbf{d}_2 \cdot \mathbf{n}(u,v) &= .2473084209 \cdot 10^{-1} \cdot u^3 + .1704287041 \cdot u^2 \cdot v \\ &\quad + .1896966327 \cdot u \cdot v^2 + .7738813204 \cdot v^3 \\ &\quad - .8009626039 \cdot u^2 - .1924457148 \cdot u \cdot v - \\ &\quad 2.618359451 \cdot v^2 + .27490821 \cdot 10^{-2} \cdot u \\ &\quad - 7.321609445 \cdot v + 5.753859446 \\ &= 0, \\ \mathbf{d}_3 \cdot \mathbf{n}(u,v) &= -.2493175219 \cdot 10^{-1} \cdot u^3 - .1898117691 \cdot u^2 \cdot v \\ &\quad - .4147900181 \cdot u \cdot v^2 - 1.473261392 \cdot v^3 \\ &\quad + .8203456689 \cdot u^2 + 1.439116772 \cdot u \cdot v \\ &\quad + 9.857085851 \cdot v^2 - .6260846109 \cdot u \\ &\quad - 12.72409444 \cdot v + .928041846 \\ &= 0. \end{aligned}$$

– origin (obtained as intersection of the three symmetry planes):
$\mathbf{o}(-.1876629728 \cdot 10^{-9}, .1500000000 \cdot 10^{-9}, .4500000000 \cdot 10^{-9})$.

6. Conclusion

In this paper we presented a geometric method for extracting the geometric invariants of a given rational quadratic quadric triangle in form of its axes. Thus, together with the algorithm from [3] it is now possible to examine a given parametric rational quadratic Bézier triangle B in order to, step by step, extract its complete geometric information in the following way:

(1) Determine whether B represents a quadric.
(2) If yes, then, denoting the underlying quadric by Q:
   a) determine Q's projective type,
   b) determine Q's affine type,
   c) determine Q's axes directions $\mathbf{d}_1, \mathbf{d}_2, \mathbf{d}_3$,
   d) determine the position of the origin $\mathbf{o}$ such that with respect to the coordinate system $\{\mathbf{o}; \mathbf{d}_1, \mathbf{d}_2, \mathbf{d}_3\}$ Q has normal form.

The steps 2)c) and 2)d) detailed in the present paper provide new geometrical insight and have been added to the algorithm from [3], and applied to several significant examples, thus illustrating its performance.

The method is aimed at application areas where geometrical knowledge is of primary importance such as for example in CAD applications, e.g., for verifying a geometric setting or solving constrained geometric configurations, etc.

References

[1] Albrecht, G., A note on Farin points for rational triangular Bézier patches, *Comput. Aided Geom. Design* **12**, 507–512 (1995).
[2] Albrecht, G., A geometrical design handle for rational triangular Bézier patches, in *The Mathematics of Surfaces VII* (T. Goodman, R. Martin, eds.), Information Geometers Ltd., Winchester UK, 161–171 (1997).
[3] Albrecht, G., Determination and classification of triangular quadric patches, *Comput. Aided Geom. Design* **15**, 675–697 (1998).
[4] Albrecht, G.,A Practical Classification Method for Rational Quadratic Bézier Triangles with Respect to Quadrics, in *Mathematical Methods for Curves and Surfaces II*, (M. Dæhlen, T. Lyche, L. L. Schumaker, eds.), Vanderbilt Univ. Press, Nashville TN, 1–8 (1998).
[5] Albrecht, G., *Rational Triangular Bézier Surfaces — Theory and Applications*, Shaker Verlag (1999).
[6] Albrecht, G., An Algorithm for Parametric Quadric Patch Construction, *Computing*, **72**, 1–12, (2004).
[7] Boehm, W. and Hansford, D., Bézier Patches on Quadrics, in *NURBS for Curve and Surface Design* (G. Farin, ed.) SIAM, Philadelphia, 1–14, (1991).
[8] Boehm, W. and Hansford, D., Parametric representation of quadric surfaces, in *Math. Modelling and Num. Analysis 26*, No. 1, 191–200 (1992).
[9] Coffman, A., Schwartz, A.J. and Stanton, Ch., The algebra and geometry of Steiner and other quadratically parametrizable surfaces, *Comput. Aided Geom. Design* **13**, 257–286 (1996).
[10] Degen, W.L.F., The types of triangular Bézier surfaces, in *The Mathematics of Surfaces VI* (G. Mullineux, ed.), The IMA Conference Series No. 58, Clarendon Press Oxford, 153–170 (1996).

[11] Farin, G., *Curves and Surfaces for Computer Aided Geometric Design*, Academic Press Inc., Boston (1990).
[12] Gregory, J., N–sided surface patches, in *The Mathematics of Surfaces*, (J. Gregory, ed.), Clarendon Press, Oxford, 217–232 (1986).
[13] Hagen, H., Nielson, G. and Nakajima, Y., Surface design using triangular patches, *Comput. Aided Geom. Design* **13**, 895–904 (1996).
[14] Joe, B. and Wang, W.P., Reparametrization of rational triangular Bézier surfaces, *Comput. Aided Geom. Design* **11**, No. 4, 345–361 (1994).
[15] Karciauskas, K., Quadratic Triangular Bézier Patches on Quadrics, Preprint (1997).
[16] Kmetová, M., Rational quadratic Bézier triangles on quadrics, *Acta Mathematica* **2**, Faculty of Natural Sciences, University of Education, Nitra, Slovakia, 97–104 (1995).
[17] Lü, W., Rational parametrization of quadrics and their offsets, *Computing*, **57**(2), 135–147 (1996).
[18] Niebuhr, J., *Eigenschaften der Darstellung insbesondere degenerierter Quadriken mittels Dreiecks–Bézier–Flächen*, Diss. Universität Braunschweig (1992).
[19] Pascal, E.,*Repertorium der höheren Mathematik*, 2. Band (Geometrie), Teubner, Stuttgart (1910/1922).
[20] Sanchez-Reyes, J. and Paluszny, M., Weighted radial displacement: A geometric look at Bézier conics and quadrics, *Comput. Aided Geom. Design* , **17(3)**, 267–289 (2000).
[21] Sederberg, T. W. and Anderson, D. C., Steiner Surface Patches, *IEEE Computer Graphics and Applications*, 23–36 (May 1985).
[22] Theisel, H., Using Farin points for rational Bézier surfaces, *Comput. Aided Geom. Design* **16**, 817–835 (1999).
[23] Vaisman, I., *Analytical Geometry*, Series on University Mathematics Volume 8, World Scientific (1997).
[24] Varady, T., Survey and new results in n–sided patch generation, in *The Mathematics of Surfaces II*, (R. Martin, ed.), Oxford Univ. Press, Oxford, 203–235 (1987).

Univ Lille Nord de France, UVHC, LAMAV-CGAO, FR CNRS 2956, F–59313 Valenciennes, France, http://www.univ-valenciennes.fr/lamav/albrecht/
E-mail address: gudrun.albrecht@univ-valenciennes.fr